ResearchGate

See discussions, stats, and author profiles for this publication at: https://www.researchgate.net/publication/231241207

Microfocus X-ray Diffraction Study of the Columnar Phase of Porphyrin-Based Mesogens

ARTICLE *in* CHEMISTRY OF MATERIALS · OCTOBER 2007

Impact Factor: 8.35 · DOI: 10.1021/cm702063a

CITATIONS
29

READS
9

8 AUTHORS, INCLUDING:

Shin-Woong Kang
Chonbuk National University
91 PUBLICATIONS **1,149** CITATIONS
SEE PROFILE

Quan Li
The Chinese University of Hong Kong
258 PUBLICATIONS **6,677** CITATIONS
SEE PROFILE

Julie O. Cross
Argonne National Laboratory
89 PUBLICATIONS **1,860** CITATIONS
SEE PROFILE

Available from: Satyendra Kumar
Retrieved on: 31 January 2016

Microfocus X-ray Diffraction Study of the Columnar Phase of Porphyrin-Based Mesogens

Shin-Woong Kang,[†] Quan Li,[‡] Brandon D. Chapman,[||] Ron Pindak,[||] Julie O. Cross,[⊥] Langfang Li,[‡] Michi Nakata,[§] and Satyendra Kumar*,[†,#]

Department of Physics and Liquid Crystal Institute, Kent State University, Kent, Ohio 44242, Department of Physics, University of Colorado, Boulder, Colorado 80309, Brookhaven National Laboratory, Upton, New York 11973, Argonne National Laboratory, Argonne, Illinois 60439, and Division of Materials Research, National Science Foundation, 4201 Wilson Boulevard, Arlington, Virginia 22230

Received July 27, 2007. Revised Manuscript Received September 4, 2007

Porphyrin-based materials are prime candidates for solar energy harvesting applications. New compounds incorporating the porphyrin core, which exhibit the columnar liquid crystal (LC) phase, were synthesized as they offer a route to obtaining defect-free large area monodomain films. The structure of the phases exhibited by these materials has been probed by synchrotron X-ray diffraction with a microfocus (14 μm × 14 μm) beam. Exploiting the multidomain nature (i.e., having differently oriented crystal axes) of a thin glass cell, it was possible to obtain complete structural information without the need to have one single macroscopic crystal, which is normally difficult to obtain. The results confirmed the existence of the isotropic, discotic (columnar) LC, and discotic-ordered LC phases in these materials. The optical microscopic work demonstrates how macroscopic control of columnar orientations is achieved by manipulating the LC film thickness, substrate preparation, and the thermal annealing process.

Introduction

The limited efficiency of inorganic photovoltaic (IPV) cells and the high cost of semiconductor processing have limited their utility and potential impact on global energy usage. Although their efficiency has inched upward in recent years, the IPVs remain far from becoming a commercially viable alternative to the traditional fossil, hydroelectric, and nuclear sources of energy. In comparison, the organic photovoltaic (OPV) materials offer a number of advantages over the semiconductor-based route. The ease with which organic photovoltaics can be mass-produced at reasonably low cost in the form of thin, lightweight, and even flexible panels using roll-to-roll processing render them commercially and environmentally very attractive.[1]

According to a recent study,[1] a device efficiency of 10% is considered essential before they can be taken to market. Efficiencies as high as 5.7% have been demonstrated[2] for the OPV devices using C60 electrodes. It is expected that if materials can be designed to respond over the entire visible spectrum having higher absorption efficiency and the cells can be fabricated with lower series resistance, then efficiency as high as 20% is feasible at significantly lower costs, making them preferred over the IPV devices. One of the perennial problems with both inorganic and organic devices is that their efficiency is greatly limited by the presence of crystalline defects. Porphyrin derivatives exhibiting liquid-crystalline phases offer an ease of synthesis and enhanced charge collection owing to increased π-orbital overlap with C60 and carbon nanotubes materials that can be used as electrodes. The intrinsic liquid crystalline nature of these materials provides a crucial advantage toward realizing such device applications. The highly (orientationally and positionally) ordered liquid crystal phase and associated high carrier mobility due to its intrinsic phase structure makes their processing easier with more flexibility for incorporation into different device configurations.[3−5] A potential problem with these devices lies in collecting the electrons and holes generated from the photoinduced excitons, but several methods have been proposed to overcome this bottleneck.[6] It has been shown that efficiencies of up to 20% are feasible in fully optimized and configured devices. This modest efficiency combined with a low cost of production makes them highly competitive with the conventional sources of energy.

* To whom correspondence should be addressed.
[†] Department of Physics, Kent State University.
[‡] Liquid Crystal Institute, Kent State University.
[§] University of Colorado.
[||] Brookhaven National Laboratory.
[⊥] Argonne National Laboratory.
[#] National Science Foundation.

(1) (a) Special Issue on "Organic Photovoltaics". *MRS Bull.* **2005**, *30*, 1. (b) Scharber, M. C.; Muhlbacher, D.; Koppe, M.; Denk, P.; Waldauf, C.; Heeger, A. J.; Brabec, C. J. *Adv. Mater.* **2006**, *18*, 789−794.
(2) Xue, J.; Uchida, S.; Rand, B. P.; Forrest, S. R. *Appl. Phys. Lett.* **2004**, *85*, 5757−5759.
(3) Wang, Q.-M.; Bruce, D. W. *Chem. Commun.* **1996**, 2505−2506. Gregg, B. A.; Fox, M. A.; Bard, A. J. *J. Phys. Chem.* **1990**, *94*, 1586−1598. Ohta, K.; Yamaguchi, N.; Yamamoto, I. *J. Mater. Chem.* **1998**, *8*, 2637−2650.
(4) (a) Adams, D.; Closs, F.; Frey, T.; Funhoff, D.; Haarer, D.; Ringsdorf, H.; Schuhmacher, P.; Siemensmeyer, K. *Phys. Rev. Lett.* **1993**, *70*, 457−460. (b) Adams, D.; Schuhmacher, P.; Simmerer, J.; Haussling, L.; Siemensmeyer, K.; Etzbach, K. H.; Ringsdorf, H.; Haarer, D. *Nature* **1994**, *371*, 141−143.
(5) Schmidt-Mende, L.; Fechtenkotter, A.; Mullen, K.; Moons, E.; Friend, R. H.; Mackenzie, J. D. *Science* **2001**, *293*, 1119−1122.
(6) Bushby, R. J.; Lozman, O. R. *Curr. Opin. Solid State Mater. Sci.* **2002**, *6*, 569−578.

10.1021/cm702063a CCC: $37.00 © 2007 American Chemical Society
Published on Web 10/19/2007

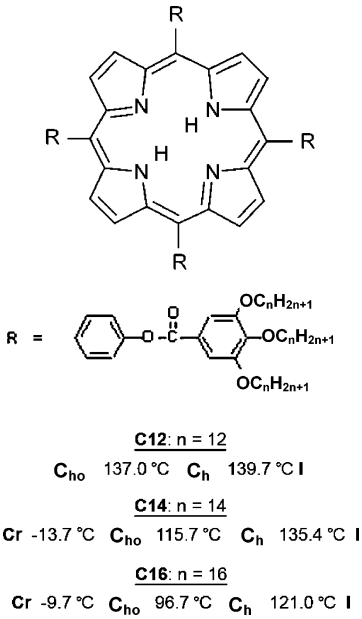

Figure 1. Molecular structures, phases, and transition temperatures for compounds **C12**, **C14**, and **C16**. I = isotropic liquid; C_h = liquid crystalline hexagonal phase; C_{ho} = ordered hexagonal phase; Cr = crystal.

Table 1. Phase Transition Temperature (°C) and Enthalpies (J/g)[a]

C12	I	139.7 (1.1)	C_h 137.0 (7.7)	C_{ho} < −50	Cr
C14	I	135.4 (2.5)	C_h 115.7 (7.3)	C_{ho} −13.7 (10.0)	Cr
C16	I	121.0 (1.9)	C_h 96.7 (−5.80)	C_{ho} 9.7 (23.0)	Cr

[a] Cooling rate, 5 °C/min; *I* = isotropic liquid; C_h = hexagonal LC phase; C_{ho} = ordered hexagonal LC phase; Cr = crystal.

In recent years, several successful attempts based on the ability to control the orientational and positional order of liquid crystalline material have been reported for OPV devices,[3] electroluminescent displays, and field effect transistors.[4−8] Both calamitic and discotic LCs are being intensively studied for this purpose. Previously, similar attempts were made using discotic columnar LCs which exhibit significantly enhanced carrier mobility along the column axis, akin to a one-dimensional semiconducting wire.[4−6] In addition to a high degree of molecular ordering within columns, the control of column orientation and domain size is crucial for enhancing device performance.[9−11] Recently, we successfully synthesized some porphyrin[12]-based discotic liquid crystalline materials with demonstrated photocurrent generation.[13]

To prepare the defect-free samples necessary for higher efficiencies, it is imperative to understand the structure and molecular organization of these materials in the LC phases. Although liquid crystals are less ordered than crystals, they provide several advantages such as the control of columnar orientation on a macroscopic scale and freedom from grain boundaries which, if present, are easier to thermally anneal compared to crystalline phases. In this regard, columnar liquid crystals are more promising due to the high degree of molecular order within columns, relatively large domain size, and high electrical conductance along the column axis. Once aligned, a liquid crystalline phase can be further cooled into the crystalline phase without losing the degree of alignment, often through an intermediate and more ordered LC phase. The cooling rate across the phase transitions can be controlled to eliminate or minimize the generation of defects. Furthermore, defect formation due to thermal contraction of the hexagonal lattice across the transition to the lower temperature phase is unlikely to disrupt the conduction path along the column axis and may not prove detrimental to electrical conduction in this direction, or negatively influence the charge collection efficiency. In general, it is known that bigger rigid cores form highly ordered columns due to enhanced $\pi-\pi$ interactions between aromatic cores.[6,14] However, in this case, the control of orientational order of discotic columns becomes more challenging. Toward this end, we have performed a study of the alignment and structure of three porphyrin-based mesogens in bulk and in

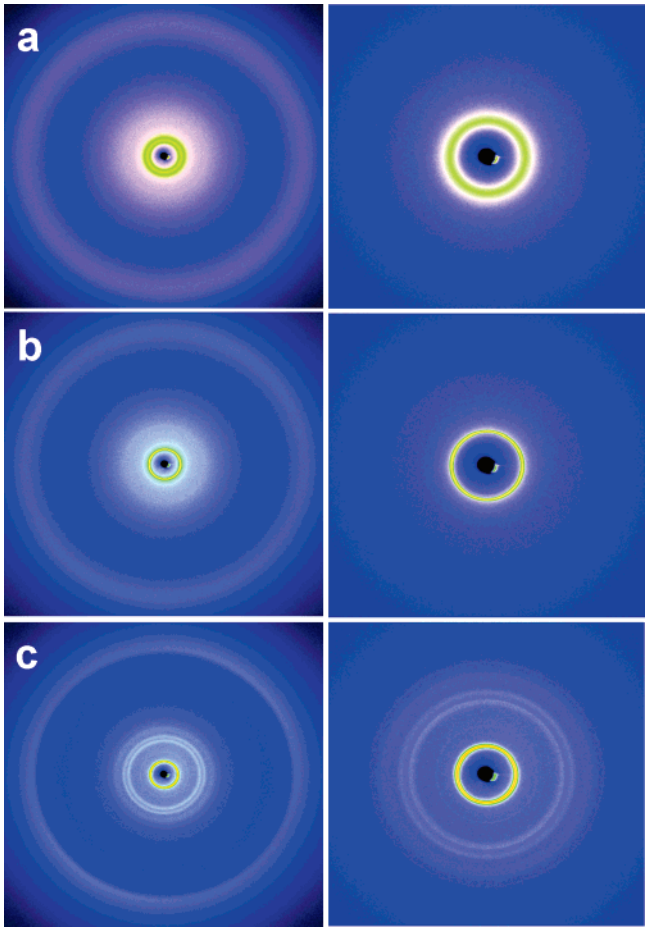

Figure 2. Powder X-ray diffraction patterns of sample **C16**. The panels on the right show the small-angle scattering at a high magnification. (a) Isotropic phase at 132.0 °C, (b) LC Ch phase at 119.0 °C, and (c) C_{ho} phase at 87.0 °C.

(7) Forester, S. R. *Mater. Res. Soc. Bull.* **2005**, *30*, 28−32.
(8) O'Neill, M.; Kelly, S. M. *Adv. Mater.* **2003**, *15*, 1135−1146.
(9) Bushby, R. J.; Lozman, O. R. *Curr. Opin. Colloid Interface Sci.* **2002**, *7*, 343−354.
(10) Percec, V.; Glodde, M.; Bera, T. K.; Miura, Y.; Shiyanovskaya, I.; Singer, K. D.; Balagurusamy, V. S. K.; Heiney, P. A.; Schnell, I.; Rapp, A.; Spiess, H.-W.; Hudson, S. D.; Duan, H. *Nature* **2002**, *419*, 384.
(11) Shiyanovskaya, I.; Singer, K. D.; Percec, V.; Bera, T. K.; Miura, Y.; Glodde, M. *Phys. Rev. B* **2003**, *67*, 035204.
(12) Eichhorn, H. *J. Porphyrins Phthalocyanines* **2000**, *4*, 88.
(13) Li, Q.; Jakli, A. et al., unpublished results.
(14) (a) Christopher, A. H.; Jeremy, K. M. S. *J. Am. Chem. Soc.* **1990**, *112*, 5525−5534. (b) Ban, K.; Nishizawa, K.; Ohta, K.; van de Craats, A. M.; Warman, J. M.; Yamamoto, I.; Shirai, H. *J. Mater. Chem.* **2001**, *11*, 321−331.

thin films using optical and microfocus synchrotron X-ray scattering.

In this paper, we describe the phase behavior of novel mesomorphic porphyrin derivatives with an extended rigid core and flexible alkyl groups in their periphery. The phase structures are examined by microfocus synchrotron X-ray diffraction together with conventional X-ray powder diffraction. Furthermore, the control of orientational order of discotic columns on a macroscopic scale is achieved by manipulating the film thickness and using proper thermal treatments, substrate preparation, and mechanical shearing.

Experimental Section

The experimental details of the material synthesis are described in ref 15. For the conventional X-ray powder diffraction measurements, three homologues of mesomorphic porphyrin derivatives were loaded into 1.5 mm diameter Lindéman capillaries with 10 μm thick walls and exposed to synchrotron X-rays (0.7653 Å) at sector #6 of the Advanced Photon Source (APS) at Argonne National Laboratory. The diffraction patterns were recorded at different temperatures during cooling from the isotropic phase using a high-resolution (MAR345) area detector placed at a distance of 527.8 mm from the sample. The data were calibrated against a silicon standard (NIST 640C).

To take advantage of multiply oriented domains of these materials that naturally form in thin flat cells, microdiffraction experiments were performed using 16 keV X-rays at the bending magnet beamline of Sector #20 at the APS. The samples were sandwiched between 50 μm thick bare glass plates with an 8.0 μm gap. The X-ray beam was focused to a 14 × 14 μm size using Kirkpatrick-Baez mirrors. The sample cell was mounted inside an Instec Hot Stage that controlled the sample temperature to ±0.02 °C. The translation stages of the hot stage were motorized so the sample could be scanned transverse to the X-ray beam. An illuminator and a polarizing microscope with a video camera were mounted on a fixture that could be translated to view the sample when the X-ray beam shutter was closed. To locate the position of the X-ray beam on the sample, a thin gold aperture was mounted over the sample cell and, with the polarizing microscope removed, was scanned horizontally and the transmitted X-ray intensity was measured to set the aperture at the horizontal beam position. The polarizing microscope was then reinserted and the aperture position was noted on the video monitor and the procedure repeated for the vertical direction. This procedure located the X-ray beam position on the video monitor and the sample could then be translated so the X-ray beam would be incident on a region of interest. Domains of different brightness and color, and thus different orientation, were selected for X-ray analysis. The hot stage and video polarizing microscope assembly were mounted on a Huber kappa goniometer so the sample orientation could be scanned to match the X-ray diffraction condition. The diffraction patterns of various monodomains were collected by a Bruker CCD area detector and the data were analyzed using the software package FIT2D developed by A. P. Hammersley[16] of the European Synchrotron Radiation Facility.

Polarizing optical microscopy (POM) was done using an Olympus BX51 microscope and Mettler FP82HT hot stage for the samples in conventional electro-optic cells with different surface treatments and thicknesses. The cells were prepared with bare glass substrates, indium-tin-oxide (ITO) coated glass, and glass with specific polyimide treatments known to induce either planar or homeotropic alignment of conventional rodlike LC molecules. Uniform sample thickness was maintained at 1.8, 8.0, and 12 μm using either patterned polymer or glass fiber spacers. These samples were used to study the control of orientational order of hexagonal columns on a macroscopic scale. Conoscopy was utilized to confirm the orientation of the optic axis as a function of temperature. Differential scanning calorimetry (DSC) measurements were made with a Perkin-Elmers DSC-VII calorimeter.

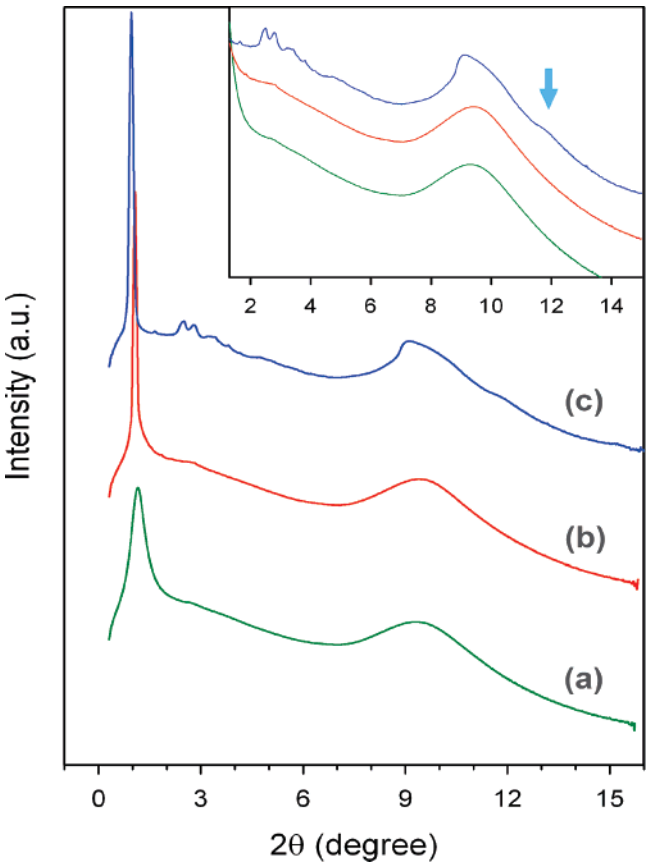

Figure 3. X-ray (λ = 0.7653 Å) intensity vs diffraction angle plots for compound **C16**: (a) isotropic phase at 132.0 °C, the two peaks correspond to 4.7 and 38.2 Å; (b) the C_h LC phase at 119.0 °C, the small-angle peak corresponds to 41.08 Å; and (c) the C_{ho} LC phase with short-range intracolumnar positional order at 87.0 °C. The fwhm of a small-angle peak are equal to (a) 0.34°, (b) 0.05°, and (c) 0.05°. The inset shows a high magnification of the plots. The arrow indicates the peak at 3.7 Å corresponding to the typical length scale of $\pi-\pi$ stacking of discotic molecules.

Results and Discussion

Chemical structures of the compounds used in this study are presented in Figure 1. The rigid core of discotic porphyrin molecules is extended and the length of flexible alkyl chains in peripheral positions was modified as shown in the figure. The phases and transition temperatures shown in Table 1 were determined by X-ray diffraction and differential scanning calorimetry during cooling at a rate of 5 °C/min. All transitions are reversible but all transitions are first-order and exhibit significant hysteresis.

The results of powder X-ray investigations for sample **C16** are shown in Figures 2 and 3. The diffraction patterns

(15) Li, L. Synthesis and characterization of nanoscale porphyrin based liquid crystals for organic photovoltaic applications. MS Thesis, Kent State University, 2005.

(16) Hammersley A. P.; Hanfland M.; Fitch A. N.; Häusermann, D. *High Pressure Res.* **1996**, *14*, 235−248.

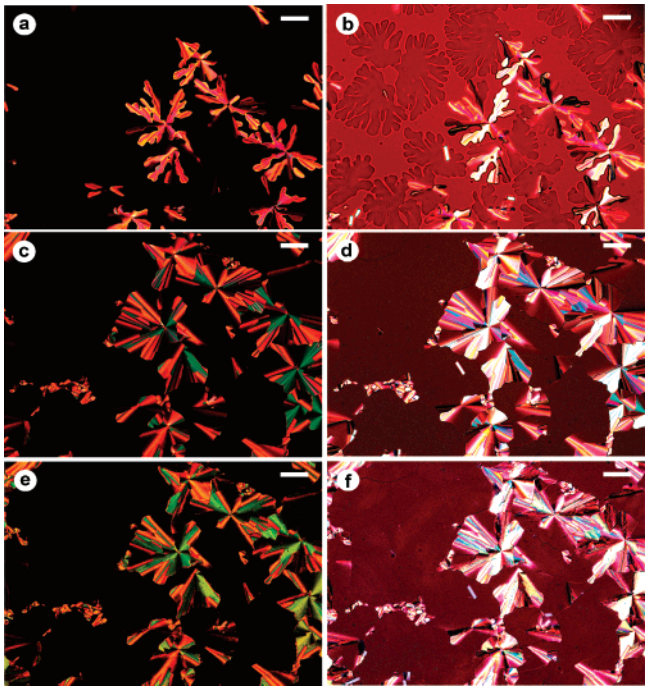

Figure 4. Optical textures for the microdiffraction from **C16** in a 8.0 μm thick glass cell. The images were taken at the same location with two different analyzer orientations: left, 90°; right, 70° between the polarizers; (a,b) 120.2 °C, (c,d) 110.0 °C, and (e,f) 36.0 °C. The scale bar corresponds to 50 μm.

obtained at 132.0 °C consists of two diffused rings at large and small angles corresponding to 4.7 and 38.2 Å, respectively, indicating the presence of the isotropic phase. The small-angle peak is more condensed than that in the isotropic phase of conventional mesogens. It has a full-width at half-maximum, fwhm, of 0.34°, which corresponds to a positional order correlation length of 130 Å, or more than three molecular dimensions. It underlines the presence of short-range order beyond the first neighbor molecule. The inner ring corresponding to 41.08 Å becomes significantly condensed (fwhm = 0.05°) at 119 °C while the outer ring retains the diffuse liquid-like shape, indicating the formation of a liquid crystalline discotic or columnar LC phase (C_h) with hexagonal structure. In the C_h phase, the side chains are disordered and there is liquid-like intracolumn positional order. Below 96.7 °C, the side chains become somewhat ordered and the intracolumn positional order grows but remains short range as suggested by the wide large-angle peak. In this phase, intercolumn positional order becomes long-range as attested to by the presence of numerous sharp small-angle peaks. This phase, to which we refer as the (more) ordered columnar phase, or C_{ho}, appears over a wide temperature range prior to crystallization. Figures 2c and 3c reveal more subtle features corresponding to the intercolumnar correlations in the small-angle region. Although it macroscopically behaves as sticky paste, this phase clearly possesses weak positional order of disks along the column axis; i.e., it is a more ordered phase than the columnar LC phase. The intensity vs 2θ plot has a well-defined peak at 3.7 Å (marked by the arrow in the inset of Figure 3) corresponding to the typical distance for $\pi-\pi$ stacking of discotic molecules. A similar phase was previously reported in other discotic liquid crystal systems.[17]

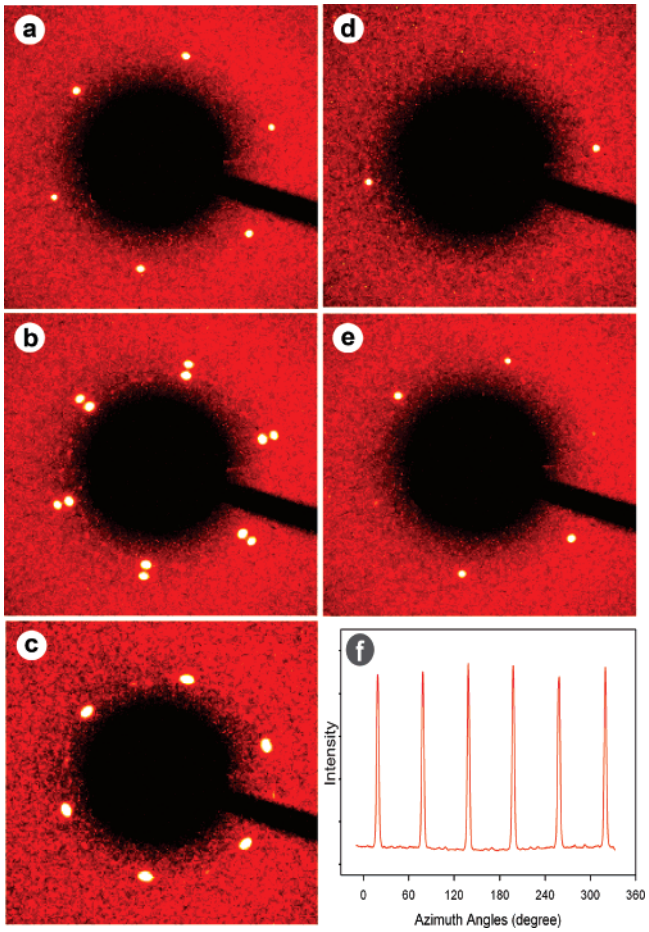

Figure 5. X-ray diffraction patterns from microscopic monodomains of **C16** in a 8.0 μm cell. The hexagonal columnar structures in the (a) LC C_h phase at 109.0 °C, (b) coexisting C_h and C_{ho} phases with different crystal modifications at 103.0 °C. The inner and outer sets of hexagonal patterns correspond to the C_h [38.2 Å] and C_{ho} [41.02 Å] phases at 75.0 °C. (c) the C_{ho} phase [41.02 Å] at 75.0 °C. (d) and (e) represent additional patterns for planar and slightly tilted domains, respectively, observed in the LC phase at 114.0 °C. (f) The azimuthal scan of the peak in (c) shows equally spaced six peaks with uniform intensity distribution.

Although all samples displayed the same mesomorphic phase between the isotropic and the crystalline phase, the powder patterns (i.e., radial isotropic distribution of diffracted intensity) display no evidence of the macroscopic alignment of discotic columns. Very similar diffraction patterns were obtained from compound **C14**. In **C14**, a weak orientational anisotropy is seen in the pattern due to flow-induced partial alignment of the discotic columns (see Figure S2 in the Supporting Information).

Figure 4 shows the POM textures at different temperatures which were used in the microdiffraction experiment on compound **C16**. The optically birefringent domains slowly grow in a dark background slightly below the transition from the isotropic phase (Figure 4a). The slow growth of optically dark, homeotropically oriented domains is also visible in Figure 4b, when the analyzer is uncrossed with the polarizer. Conoscopy observations and the results of X-ray microdiffraction both confirm homeotropic orientation. Once the

(17) (a) Fontes, E.; Heiney, P. A.; de Jeu, W. H. *Phys. Rev. Lett.* **1988**, *61*, 1202−1205. (b) Heiney, P. A.; Fontes, E.; de Jeu, W. H.; Riera, A.; Carroll, P.; Smith, A. B. *J. Phys. France* **1989**, *50*, 461−483.

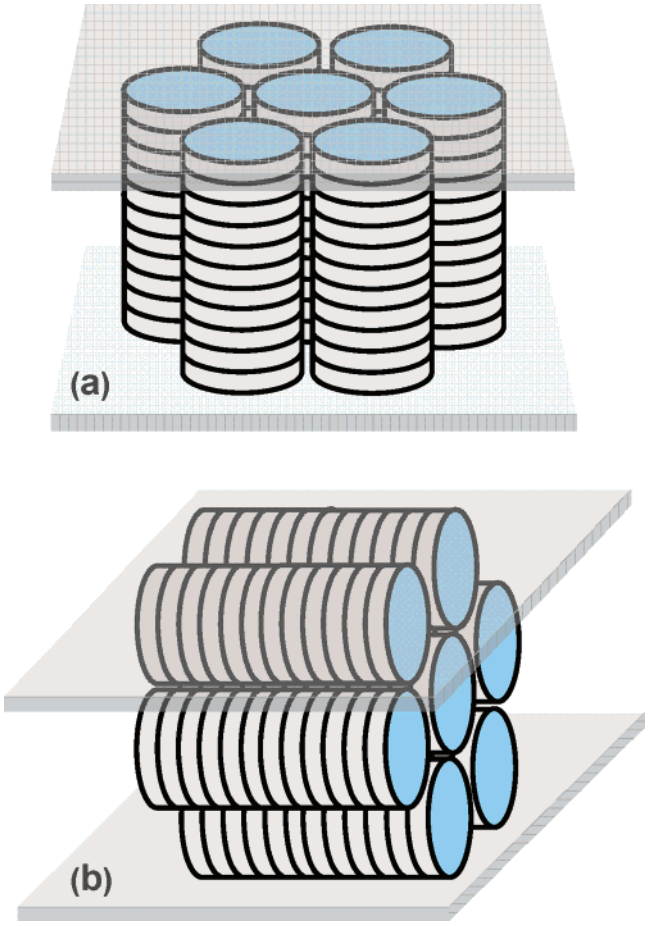

Figure 6. Schematic representation of hexagonal columnar structures in (a) homeotropic and (b) planar or homogeneous orientations with respect to the substrates.

transition from the isotropic phase to the columnar phase is complete, no significant changes in POM textures occurred at the transition to the lower temperature C_{ho} phase, as shown in Figures 4c−4f. The microfocused X-ray beam was directed at different domains in different phases while using optical textures as a guide. X-ray diffraction from an optically dark homeotropic domain is shown in Figure 5a. It represents a uniformly aligned hexagonal structure of discotic columns. During the transition to the C_{ho} phase, only the diffraction angle (i.e., the *d*-spacing) was found to change. The azimuthal orientation of the peaks, i.e., the direction of the hexagonal axes, remained the same as that in Figure 5a. This is obvious from a comparison of the patterns in Figures 5a and 5c. The columnar C_h and the C_{ho} phases coexist during the heating cycle as evident from Figure 5b (see more details in Figure S1). The azimuthal scan of the diffraction pattern reveals 6-fold symmetry of the diffraction peaks with uniform intensity distribution, in Figure 5f, indicating that the dark areas consist of a homeotropically oriented columnar phase. In addition, the diffraction patterns from a domain with planar (Figure 5d) and tilted configuration (Figure 5e) were obtained by focusing the beam on microdomains with different brightness. Figure 6 schematically depicts two types of arrangement of the hexagonal columns. Figures 6a and 6b show the homeotropic and planar orientation of the hexagonal columns, respectively. Diffraction patterns corresponding to these domains are shown in Figures 5a/5c and 5d.

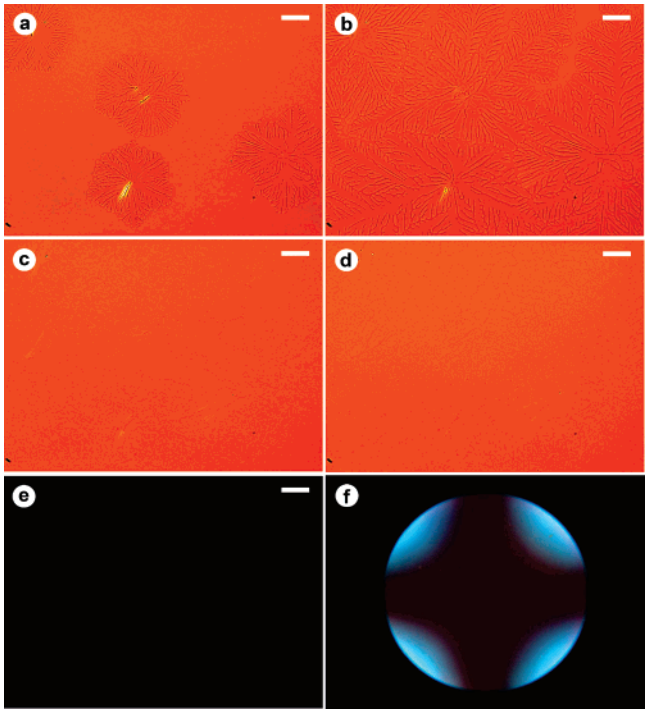

Figure 7. Formation of homeotropic texture on a macroscopic scale via slow cooling of the 1.8 μm cell with **C16**. Slow cooling induces selective nucleation and growth of homeotropic domain (parts (a) and (b) at 121.0 °C) and hence yields uniform homeotropic columnar orientation at lower temperatures ((c) 113.0 °C and (d) 75.0 °C), confirmed by both (e) optical texture under crossed polarizers and (f) conoscopic image at 75.0 °C. Optical images were taken at (a−d) 70° and (e) 90° angles between polarizers. The scale bar corresponds to 50 μm.

Similar results were obtained for compounds of **C12** and **C14**. The change in *d*-spacing between the C_{ho} and C_h liquid crystalline hexagonal phases of the **C14** was clearly captured via the coexistence of these phases during heating with no observable change in the orientation of hexagonal axes (Figure S2 in the Supporting Information).

The ability to control the macroscopic orientation of the column axis with respect to the bounding surfaces of the cell is crucial as it determines the efficiency of solar energy harvesting devices. In general, increasing the size of the aromatic core of the discotic molecules is found to enhance their tendency to pack into columns with higher carrier mobility along the column axis.[6,14] But readily acquiring uniform column orientation has been a challenge.[6,14] To devise ways to control and improve alignment uniformity, three parameters (film thickness, surface preparation/modification, and thermal history/treatment) were varied to determine their effect on the orientational order of column axes on flat solid surfaces. Various surfaces such as bare glass, ITO-coated glass, and polyimide-coated glass with and without mechanical rubbing were used. Conditions known to yield planar or homeotropic anchoring of conventional calamitic LC molecules were tested in cells with 12.0, 8.0, and 1.8 μm gaps. The rates of cooling from the isotropic phase and annealing at specific temperatures were varied and their effects on the alignment and uniformity were determined. Our results show that surface modification was not necessary for obtaining uniform homeotropic alignment. The

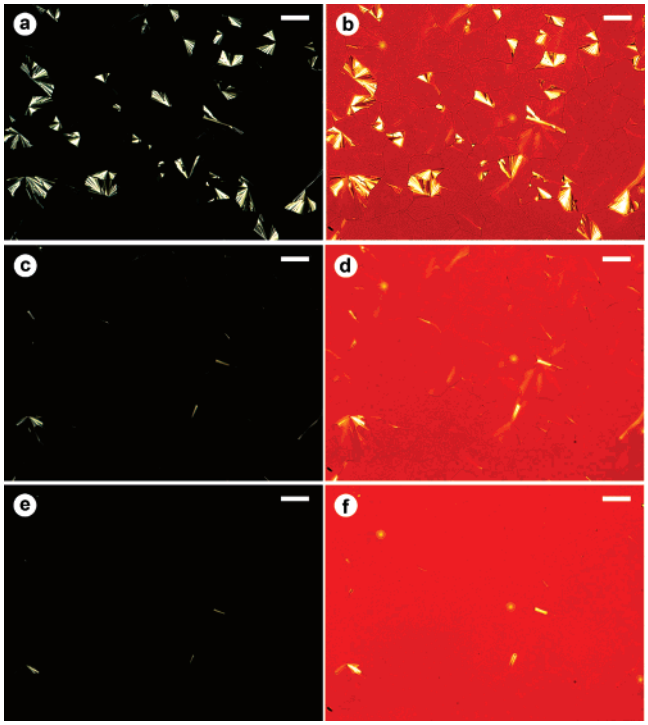

Figure 8. Spontaneous transition from planar to homeotropic orientation observed for compound **C16** in a 1.8 μm cell. The planar domains (a,b) obtained upon fast cooling slowly transform to (c,d) the homeotropic state during annealing at 113.0 °C for 2 h. Annealing at higher temperature (118.0 °C for 20 min) accelerates the process (e,f). Optical images were taken at (a, c, e) 90° and (b, d, f) 70° angles between the polarizers. The scale bar corresponds to 50 μm.

dominant factors in determining the macroscopic uniformity are the film thickness and thermal treatment. Thinner cells resulted in more uniform textures for all samples. Figure 7 illustrates the formation of uniform texture for compound **C16** confined in a 1.8 μm thick cell with polyimide coatings (which normally yield homeotropic alignment for rodlike mesogens). Slow cooling at a rate of 0.1 °C/min from the isotropic phase resulted in selective nucleation and slow growth of homeotropic domains while abrupt cooling created multidomain structure. Optical textures, with polarizer and analyzer at an angle of 70°, revealed dendritic growth of the homeotropic domains below the transition from the isotropic phase. These areas gradually grew and eventually filled the entire cell, i.e., ~1 cm × 1 cm. The optical image became and remained uniformly featureless at lower temperature, as shown in Figure 7c in the C_h phase at 113.0 °C and Figure 7d in the C_{ho} phase at 75.0 °C. A completely dark appearance under crossed polarizers (Figure 7e) and the symmetric cross in the conoscopic image (Figure 7f) confirm that the optic axis was parallel to the direction of light's propagation (i.e., the axis of the hexagonal phase was perpendicular to the cell surface).

The effect of thermal treatment varied with the compound used. Sample **C14** and **C16** were similar while **C12** acted differently (see Figure S3 in the Supporting Information). For **C12** (see Figures S4 and S5), the initial homeotropic domains obtained upon slow cooling were replaced by new strongly birefringent domains due to mostly tilted misorientation of the column axis. This is probably due to a very narrow temperature range of the LC phase. In this case, fast cooling soon after the start of the nucleation of homeotropic

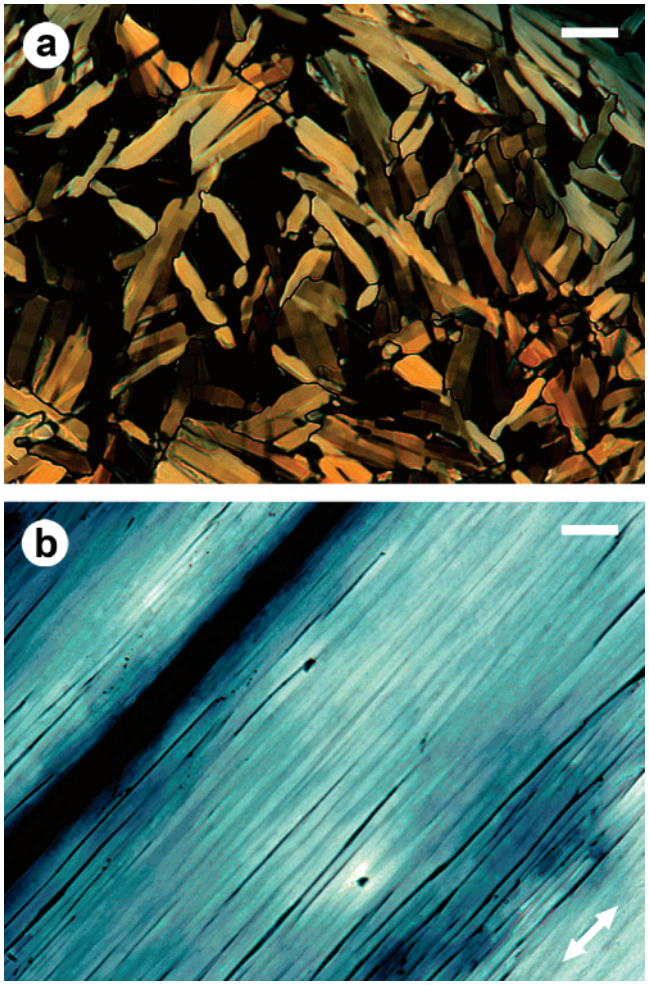

Figure 9. POM textures for thin films of compound **C12** on a single substrate. (a) Randomly oriented planar domains formed without shearing, and (b) highly ordered planar texture where the hexagonal columns are aligned along the shear direction. The double-ended arrow represents a shear direction. The scale bar corresponds to 25 μm.

domains suppressed the formation of birefringent domains and resulted in a uniform homeotropic state (Figure S6, Supporting Information).

In the LC phase, these materials exhibit a tendency to self-heal whereby defects in **C14** and **C16** give way to a homeotropic configuration upon annealing. The strongly birefringent domains in Figures 8a and 8b, obtained during fast cooling of **C16**, slowly transformed into a homeotropic state (Figures 8c and 8d) when annealed at 113.0 °C for 2 h. This healing process accelerated at higher temperatures. The homeotropic texture became more uniform when the cell was annealed at 118.0 °C for 20 min, Figures 8e and 8f. However, compound **C12** possesses a very narrow LC phase and appears to behave in a contrary manner and annealing results in the appearance of new defects, i.e., more birefringent domains.

The preferential anchoring of these porphyrin-based mesogens seems to be homeotropic. It is well-known that in the nematic phase this type of molecule (i.e., discotic) generally prefers to lie flat on the surface. The growth of columnar structures near the substrate surface enhances homeotropic alignment. However, one expects the columns to nucleate with random orientations in the bulk or in thick films away from cell walls (i.e., in the absence of any surface

anchoring). In thin cells, on the other hand, the effect of surface anchoring may permeate the entire cell thickness and produce better homeotropic configuration.

A uniform planar state of the column axis can be obtained by mechanical shearing of the sample cell. Figure 9 shows a thin **C12** film deposited on a single substrate without and with mechanical shearing. The optical texture in Figure 9a displays multiple homeotropic and randomly oriented planar domains. On the other hand, a sample film that was sheared and annealed near the isotropic transition shows a uniformly aligned planar state in Figure 9b. The columns are clearly aligned parallel to the shear direction indicated by the double arrow. This film shows maximum brightness at 45° with respect to the polarizer/analyzer axis. The dark areas in Figure 9b correspond to voids.

Conclusions

The results presented here unambiguously show hexagonal columnar structures in both the C_h and C_{ho} phases. The flat rigid core of these molecules promotes the formation of highly aligned columnar phase near flat substrates. The surface treatments used for conventional rodlike LC molecules essentially have no effects on the orientation of the columns axis of the LC phase. The dominant factors responsible for the formation of a uniform macroscopic homeotropic state are the thickness and thermal processes. In addition, the dynamic nature of LC phase and the anchoring effect of solid substrates conspire and provide a self-repairing mechanism leading to the formation of a homeotropic alignment in thin cells. Clearly, these properties of mesomorphic porphyrin derivatives place them among the most promising candidates for organic photovoltaic applications.

Acknowledgment. This work was supported, in part, by the National Science Foundation Grant DMI-0423619, by an Ohio Board of Regents' Research Challenge award, and by DOE NSET Grant No. 04SCPE389 (R.P. and B.D.C.). Use of the Advanced Photon Source (APS) was supported by the U.S. Department of Energy (DOE), Basic Energy Sciences (BES), Office of Science, under Contract No. W-31-109-Eng-38. The Midwestern Universities Collaborative Access Team's (MU-CAT) sector at the APS is supported by the U.S. DOE, BES, Office of Science, through the Ames Laboratory under Contract No. W-7405-Eng-82. PNC/XOR facilities at the Advanced Photon Source, and research at these facilities, are supported by the U.S. Department of Energy−Basic Energy Sciences, a major facilities access grant from NSERC, the University of Washington, Simon Fraser University, the Pacific Northwest National Laboratory and the Advanced Photon Source. Use of the Advanced Photon Source is also supported by the U.S. Department of Energy, Office of Science, Office of Basic Energy Sciences, under Contract DE-AC02-06CH11357.

Supporting Information Available: Microfocus X-ray diffraction patterns of the coexisting C_h and C_{ho} LC phases for sample **C16**, powder X-ray diffraction patterns of the coexisting C_h and C_{ho} LC phases for compound **C14**, optical textures formed by different thermal treatments for compound **C14**, polarizing optical images for fast cooling of the sample **C12**, optical textures for sample **C12** in 1.8 μm cell with slow cooling, uniform homeotropic texture achieved by the combination of slow and fast cooling of sample **C12** in a 1.8 μm cell. This material is available free of charge via the Internet at http://pubs.acs.org.

CM702063A